Applied Physics Letters

Electro-optic polymer/TiO_2 multilayer slot waveguide modulators

Cite as: Appl. Phys. Lett. **101**, 123509 (2012); https://doi.org/10.1063/1.4754597
Submitted: 02 July 2012 • Accepted: 10 September 2012 • Published Online: 21 September 2012

Y. Enami, B. Yuan, M. Tanaka, et al.

Electro-optic polymer/TiO_2 multilayer slot waveguide modulators

Y. Enami,[1,a)] B. Yuan,[1] M. Tanaka,[1] J. Luo,[2] and A. K.-Y. Jen[2]
[1]*Research Institute for Nanodevice and Bio Systems, Hiroshima University, Higashi-Hiroshima, Hiroshima 739-8527, Japan*
[2]*Department of Material Science and Engineering, University of Washington, Seattle, Washington 98195-2120, USA*

(Received 2 July 2012; accepted 10 September 2012; published online 21 September 2012)

We report an all-dielectric electro-optic (EO) polymer/TiO_2 multilayer slot waveguide modulator with low optical insertion loss for high-speed operations. The EO polymer is sandwiched between thin TiO_2 slot waveguide films to improve mode confinement in the EO polymer. The structure increased the mode confinement in the TiO_2 and EO polymer slot layers and reduced the electrode distance between the Au electrodes without introducing optical loss from the metal electrodes. The half-wave voltage of the modulator was 6.5 V for a 5-mm-long electrode at a wavelength of 1550 nm. The half-wave voltage and length product was 3.25 V·cm. © *2012 American Institute of Physics*. [http://dx.doi.org/10.1063/1.4754597]

Electro-optic (EO) polymer modulators have demonstrated wide 3-dB bandwidths of up to 113 GHz[1] because of their low dielectric dispersion, which is less than one tenth of the dispersion of semiconductors and $LiNbO_3$. Hybrid EO polymer/sol-gel modulators have the highest poling efficiency (~100%) for the in-device poling of EO polymers because of the high electrical conductivity of the sol-gel silica cladding layers underneath the EO polymer layer. Hybrid EO polymer/sol-gel silica waveguide modulators have the highest in-device EO coefficient of 142–170 pm/V[2] and the lowest half-wave voltage (V_π) of 0.65 V[3] in Mach–Zehnder (MZ) waveguide structures because of their high poling efficiency, with relatively lower optical insertion losses of 18 dB and 20 dB for the transverse electric (TE) and transverse magnetic (TM) modes, respectively. EO polymers and silicon are suitable candidate materials for optical modulators in future on-chip optical interconnections at a wavelength of 1.55 μm because they are non-bulky waveguide modulators that can be integrated easily with most widely commercialized complementary metal-oxide-semiconductor (CMOS) circuits. Si modulators demonstrate a 3-dB bandwidth of 13 GHz and a half-wave voltage and length product ($V_\pi L$) of 1.4 V·cm for a 1-mm-long device,[4] with an optical absorption loss of 19 dB/cm in the active region. EO polymers have been used in Si-based waveguides as cladding materials on Si_3N_4[5] cores and between Si slot waveguides.[6] The Si-EO polymer slot MZ waveguide modulator described in Ref. 6 has a V_π of 0.69 V, a 6-dB bandwidth of 500 MHz, and an optical propagation loss of 30 dB for a 1-cm-long device when the coupling loss is ignored. The optical absorption loss in the Si-EO polymer coplanar slot ring resonator waveguide of a modulator was 35 dB/cm,[7] which is the lowest value reported for a Si slot-EO polymer waveguide; however, the loss must be reduced further for practical applications with CMOS circuits. These devices usually use a grating coupling and prevent standard fiber butt coupling because of the large mode field mismatch between the fibers and modulators. Because of the lower poling efficiency of EO polymers when compared with our previous hybrid EO polymer/sol-gel silica waveguide modulators,[2,3] the highest in-device EO coefficient for EO polymers in coplanar Si–EO polymer slot waveguides was limited to 59 pm/V.[8]

Additionally, the dielectric constant of TiO_2 was higher (i.e., >30) than that of the EO polymers used (e.g., ~2). When the TiO_2 thin layer was used with an EO polymer layer, the enhanced effective field in the EO polymer layer reduced V_π. Butt coupling is the preferred waveguide-to-waveguide and fiber-to-waveguide coupling method for device packaging with single-mode (SM) fibers and integration with CMOS circuits, without the use of grating couplers[6] that have dependence of its coupling efficiency on the incident angle. Here, we report an EO polymer/TiO_2 multilayer slot waveguide modulator. To realize the potential of EO polymers for large 3-dB bandwidths of more than 100 GHz, we used metallic upper and lower electrodes rather than the previously demonstrated highly doped Si electrodes.[4–8] This slot waveguide approach aims to reduce V_π and optical insertion loss while maintaining a large 3-dB bandwidth.

EO polymer/high-index multilayer slot waveguide modulators of a MZ channel (type I) were fabricated using TiO_2 thin-film layers, as shown in Fig. 1. An organosilicate sol-gel solution was prepared for the waveguide cladding layers that consisted of methacryloyloxy propyltrimethoxysilane (MAPTMS) and an index modifier (zirconium(IV)-*n*-propoxide) with a molar ratio of 95(MAPTMS)/5 mol. %. A 0.1 M solution of HCl was used as a catalyst, and Irgacure 184 (Ciba) was used as the photoinitiator to accelerate the hydrolysis of silica for subsequent wet etching in isopropanol. Lower claddings with thicknesses of 910 nm to 4 μm were examined and coated on a 100-nm-thick Ti or Au (100 nm)/Cr (5 nm) lower electrode/silica (6 μm)-on-silicon substrate, and they were baked at 150 °C for 1 h. A side cladding layer was spin-coated on the lower cladding, and mercury i-line (365 nm) radiation in a mask aligner was delivered to the sol-gel layer through a photomask. The radiation accelerated the hydrolysis of the sol-gel silica in the exposed regions and cross-linked the silica network. The parts irradiated with

a)Electronic mail: yenami@hiroshima-u.ac.jp.

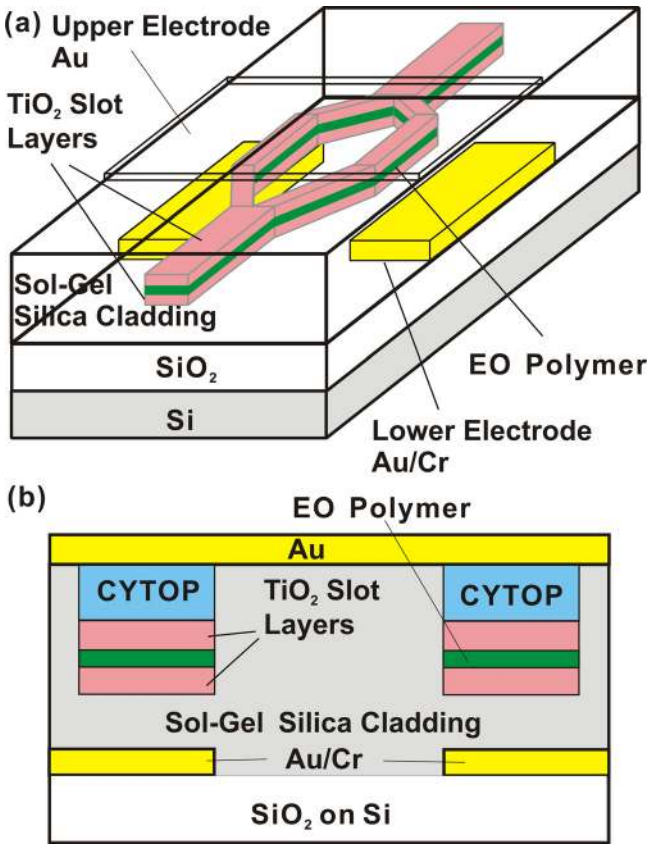

FIG. 1. Schematic cross section of the EO polymer/TiO_2 multilayer slot waveguide modulator. (a) Bird's eye view. (b) Cross-sectional view of the active region.

ultraviolet (UV) light became insoluble in isopropanol, which was used as the etchant in the wet-etching process.

The side cladding was wet etched to create a 4-μm-wide window for the EO polymer/TiO_2 multilayer slot core. After the sol-gel silica waveguide was hard-baked, a 100-nm-thick TiO_2 layer was sputtered as a lower slot core layer between the etched sol-gel side cladding layers on the lower cladding. The low-index EO polymer SEO125 (35 wt. % chromophore doped in amorphous polycarbonate (APC), index of 1.621 at 1550 nm) was spin-coated to form a 300-nm-thick layer and baked overnight at 80 °C in a vacuum oven. For the upper slot layer, a 100-nm-thick TiO_2 layer was sputtered. The ~500-nm-thick EO polymer/TiO_2 multilayer slot core was laterally confined by the side cladding to obtain good mode confinement. After the poling of the EO polymer, the removal of the poling electrode, and the sputtering of the upper slot layer, 0.9-μm-thick Cytop® (Asahi Glass) was coated as a buffer layer for the subsequent deposition of the Au upper electrode. The refractive indices of the sol-gel cladding, Cytop and the sputtered TiO_2 at 1550 nm were 1.487, 1.328, and 2.567 at 1550 nm, respectively.

We also examined a straight-channel slot waveguide (type II) for the optimization of the slot waveguide structure, using EO polymer cc1 (35-wt. % CLD(isophorone-protected polyene bridge)-type chromophore in APC, index of 1.631).[9] A multilayer slot waveguide composed of TiO_2/cc1/TiO_2 with a thickness of 200 nm/100 nm/200 nm was examined because this thickness for the slot waveguide has higher mode confinement, even though the poling efficiency was lower for the 100-nm-thick EO polymer than for the 300-nm-thick polymer, which requires a more efficient poling method. When a 100-nm-thick EO polymer with a 200-nm-thick lower TiO_2 layer in the modulators was poled on the sol-gel silica lower cladding without the upper TiO_2 layer, the poling voltage was maximized at 20–50 V to prevent the breakdown and cracking of these layers, which indicated a lower poling efficiency and higher V_π. Alternatively, we could routinely apply a poling voltage of 200–300 V for a 300-nm-thick EO polymer with a 100-nm-thick TiO_2 lower layer on the sol-gel silica lower cladding.

The optical waveguide mode was calculated for the proposed type I and type II slot waveguides using the three-dimensional finite difference time domain (3D FDTD) method with the device parameters given in Fig. 1; the mode is shown in Fig. 2(a). The mode profiles in the waveguide in the horizontal direction (X) and in the vertical direction (Y) are displayed in Figs. 2(b) and 2(c), respectively.

The coupling loss from the standard SM fiber SMF-28 to the waveguide was also calculated to be 6 dB using the 3D FDTD method. The mode field diameters (MFDs) in the

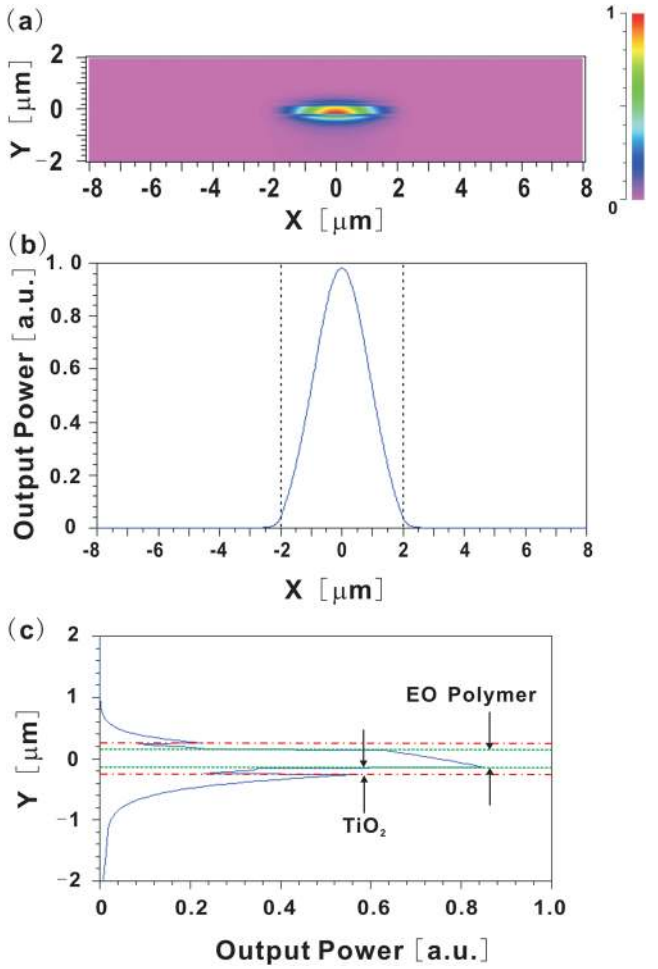

FIG. 2. Optical output mode of the EO polymer/TiO_2 multilayer slot waveguide modulator calculated using the 3D FDTD method. (a) Output mode: X, horizontal distance; Y, vertical distance. (b) The mode shape in the horizontal direction. The black dotted lines show the boundary between the multilayer slot and the sol-gel silica side cladding. (c) The mode shape in the vertical direction. The red dotted lines show the boundary between TiO_2 and the cladding, and the green dashed lines show the boundary between the EO polymer and TiO_2.

horizontal and vertical directions of the waveguide were 3.5 and 1.0 μm, respectively, and were smaller than the MFD (10.4 μm) of SMF-28 at 1550 nm. Determining the butt coupling process from a cleaved SM fiber to a SM passive Si waveguide on a SiO_2 insulator (e.g., MFD < 0.4 μm) has been challenging[10] because the coupling from the SM fiber to SM Si waveguide usually involves mode converters or grating couplers. In contrast to these active EO polymer/Si slot waveguides[5–8] and passive Si waveguides,[10] our slot waveguide enabled butt coupling while maintaining EO activity and low insertion loss. An EO modulator using this all-dielectric waveguide would have an EO modulation bandwidth (e.g., >60 GHz) larger than that of previously reported Si slot/EO polymer waveguide modulators[5–8] because of its highly conductive Au electrode (without using a highly doped Si conductor as the electrode), which is easily modified to act as a microstrip line for millimeter-wave propagation. The type II waveguide had better mode confinement, which permitted a thinner lower cladding because of the thinner EO polymer and thicker TiO_2 layers. The mode in the slot layers was calculated for type II and was confined within 2 μm in the Y direction. The index of SEO125 (1.621) was also lower than that of cc1/APC (1.631), which resulted in better mode confinement in the slot layers.

The optical output mode and insertion loss were measured for the standard SM fiber SMF-28. The input light was controlled such that the polarization state excited a TM mode in the waveguide to enable it to serve as a modulator. The input light was butt-coupled from the facet of the cleaved SMF-28 to the waveguide on a fiber positioner. The fiber was brought to within 0.1 μm of the waveguide while contact was avoided between the two ends. The optical output was collected using a 20× microscope objective lens (resolution of 2.4 μm) and focused on the CCD camera (Newport, LBP-4-USB). We observed the mode shape of the output image, as shown in Fig. 3. The optical insertion loss for the 14-mm-long MZ modulator (type I) was 24 dB in the TM mode (the electrode length L_e was also 5 mm), where the modulator had a 300-nm-thick SEO125 EO polymer between the 100-nm-thick sputtered TiO_2 multilayer slot layers on a 4-μm-thick sol-gel silica lower cladding. The insertion loss for a 5-mm-long straight-channel modulator (type II) using a thickness of TiO_2(200 nm)/cc1(100 nm)/TiO_2(200 nm) on a 910-nm-thick lower cladding was 12 dB in the TM mode (L_e = 5 mm). When the lower cladding had a thickness of less than 1 μm, the mode in the vertical direction could reach the lower electrode as shown in Fig. 2(c).

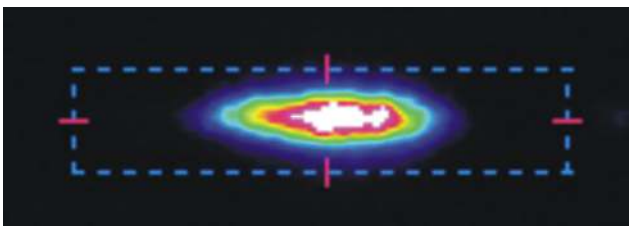

FIG. 3. Optical output from the EO polymer/TiO_2 multilayer slot waveguide. The output image was focused through a 20× microscope objective lens (numerical aperture of 0.4, effective focal length of 8.55 mm) onto a CCD camera more than 10 cm from the lens. The camera image has dimensions of 363.61 μm and 85.39 μm at full width at half maximum in the horizontal and vertical directions, respectively.

TABLE I. Optical insertion loss and device parameters.

WG	$t_{SG\ SiO_2}$[b]	t_{slot}[c]	t_{EO}[d]	L_e[e]	L_t[f]	EO	d	Loss[g]
MZ	4.0 μm	100 nm	300 nm	5 mm	14 mm	SEO125	5.4 μm	24 dB
S.C.[a]	910 nm	200 nm	100 nm	5 mm	5 mm	cc1	2.3 μm	12 dB

[a]Straight-channel waveguide.
[b]Thickness of the sol-gel silica lower cladding.
[c]Thickness of the slot layer.
[d]Thickness of the EO polymer.
[e]Length of the electrode.
[f]Total waveguide length.
[g]Optical insertion loss for the TM mode, including both the coupling loss with SMF-28 and the waveguide propagation loss.

The insertion loss is the total optical loss, which includes the coupling loss from the SMF-28 fiber to the waveguide and the waveguide propagation loss. The optimized results and the device parameters are summarized in Table I. For the MZ waveguide modulator device, the thickness of the lower cladding was increased up to 4 μm to reduce optical loss because the total length must be increased for the MZ waveguide branches.

We estimated the waveguide propagation loss to be approximately 12–13 dB/cm, which was lower than that (>35 dB/cm) for the previously reported coplanar slot Si-EO polymer waveguide modulator.[7,8] TiO_2 has a higher dielectric constant (>30) than EO polymers (~2), which also reduces the effective electrode distance in the EO modulators. These are the advantages of the proposed slot waveguide in reducing V_π. The propagation loss was less than that of previously reported Si slot/EO polymer waveguides.[5–8] From the calculated mode in the vertical direction, as shown in Fig. 2(c), and the measurement of the optical insertion loss in the waveguides, we optimized the electrode distance to prevent optical absorption from the electrodes. The thickness of the lower cladding layers must be increased to >900 nm. In the calculation shown in Fig. 2(c), there is a discontinuous mode at the boundary between TiO_2 and the EO polymer. However, the measured output mode did not show this discontinuous mode, as shown in Figs. 2(b) and 2(c), because of the limited resolution of the microscope objective lens. The calculated results inside the waveguide showed a highly confined mode in the slot waveguide and showed that reduced insertion loss in our slot waveguide was possible without concomitant optical loss from the electrodes. Additionally, the proposed slot waveguide has a lower coupling loss and propagating loss from the cleaved SMF-28 to the previous Si slot/EO polymer waveguides. The Si slot/EO polymer waveguides occasionally require mode conversion from the Si waveguide to the Si slot/EO polymer waveguide, which requires complicated mode converters and grating couplers.

The output power of the slot waveguide modulator was measured to experimentally determine V_π. The input light from the standard fiber SMF-28 to the modulator was controlled such that it was linearly polarized in the TM mode using a polarization controller and coupled into the slot waveguide in the passive region. After light propagated through

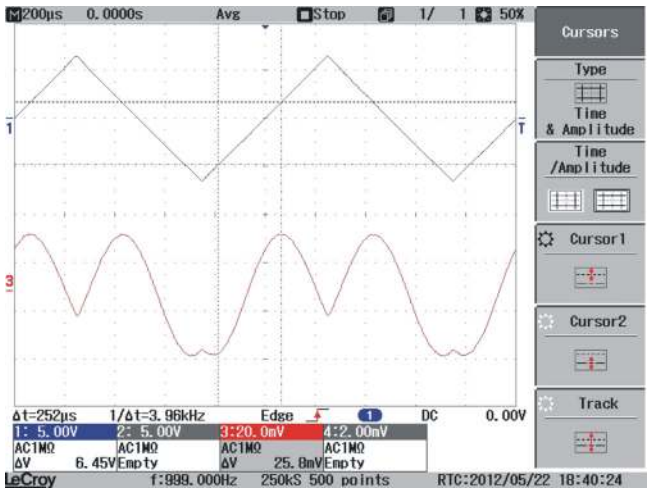

FIG. 4. Measured low-frequency transfer function at 1 kHz for the EO polymer/TiO_2 multilayer slot waveguide modulator. $V_\pi = 6.4$ V ($d = 5.4\ \mu$m, $L_e = 5$ mm) for dual-drive operation at 1550 nm. Top: Applied triangular voltage waveform. Bottom: Optical output from the modulator.

the modulator, the light output from one port was collected using the objective lens of a microscope and focused on a detector. The top electrode was grounded, and a driving voltage with opposite polarity was applied to the separated bottom electrodes. The power at the detector was monitored on an oscilloscope with an applied triangular voltage waveform, as shown in Fig. 4. The output power from the modulator was modulated with an applied voltage at a frequency of 1 kHz. From the relationship between the applied voltage and output power, a V_π of 6.5 V at 1550 nm was measured for a L_e of 5 mm ($V_\pi L_e = 3.25$ V cm) through dual-drive operation. The in-device EO coefficient was estimated to be approximately 60 pm/V at 1550 nm, and this value could be improved further by using a combination of the latest poling technique and EO polymer.

We confined and guided light through an EO polymer/TiO_2 multilayer slot waveguide. This waveguide does not require highly doped Si as the electrode for the EO modulators, which improves the bandwidth. Our multilayer slot waveguide modulators can be applied in telecommunications and as CMOS-compatible high-speed EO modulators that use a standard metal microstrip upper electrode and a metal lower electrode with lower coupling loss in the packaged or optically integrated EO modulators. When a low-index material was used as a part of the lower cladding with a total thickness of 2.4 μm, the type II insertion loss was improved to 13.9 dB (5 dB/cm). This structure should reduce V_π because of its higher mode confinement and the shorter electrode distance after the optimization of the in-device EO coefficient.

This work was supported by a Grant-in-Aid for Scientific Research (A) (Grant Nos. 21246060 and 24246063) and Grant-in-Aid for Challenging Exploratory Research (Grant No. 23651138) from the Ministry of Education, Culture, Sports, Science, and Technology, Japan, and an International Collaborative Grant from the National Institute of Information and Communications Technology, Japan (Grant No. 09150703). We also wish to thank J. Hong and Z. Huiwei in Hiroshima University.

[1]D. Chen, H. R. Fetterman, A. Chen, W. H. Steier, L. R. Dalton, W. Wang, and Y. Shi, Appl. Phys. Lett. **70**, 3335 (1997).
[2]Y. Enami, C. T. DeRose, D. Mathine, C. Loychik, C. Greenlee, R. A. Norwood, T. D. Kim, J. Luo, Y. Tian, A. K.-Y. Jen, and N. Peyghambarian, Nat. Photonics **1**, 180 (2007).
[3]Y. Enami, D. Mathine, C. T. DeRose, R. A. Norwood, J. Luo, A. K.-Y. Jen, and N. Peyghambarian, Appl. Phys. Lett. **91**, 093505 (2007).
[4]N.-N. Feng, S. Lian, D. Feng, P. Dong, D. Zheng, H. Liang, R. Shafiiha, G. Li, J. E. Cunningham, A. V. Krishnamoorthy, and M. Asghari, Opt. Express **18**, 7994 (2010).
[5]B. A. Block, T. R. Younkin, P. S. Davis, M. R. Reshotko, P. Chang, B. M. Polishak, S. Huan, J. Luo, and A. K.-Y. Jen, Opt. Express **16**, 18326 (2008).
[6]R. Ding, T. Baehr-Jones, W.-J. Kim, A. Spott, M. Fournier, J.-M. Fedeli, S. Huang, J. Luo, A. K.-Y. Jen, L. Dalton, and M. Hochberg, J. Lightwave Technol. **29**, 1112 (2011).
[7]M. Gould, T. Baehr-Jones, R. Ding, S. Huang, J. Luo, A. K.-Y. Jen, J.-M. Fedeli, M. Fournier, and M. Hochberg, Opt. Express **19**, 3952 (2011).
[8]X. Wang, C.-Y. Lin, S. Chakravarty, J. Luo, A. K.-Y. Jen, and R. T. Ray, Opt. Lett. **36**, 882 (2011).
[9]Y. Enami, J. Hong, C. Zhang, J. Luo, and A. K.-Y. Jen, IEEE Photon. Technol. Lett. **23**, 1508 (2011).
[10]Y. A. Vlasov and S. J. McNab, Opt. Express **12**, 1622 (2004).